Fortschritte der Physik

www.fp-journal.org

Progress of Physics

WILEY-VCH

Fortschr. Phys. **61**, No. 2 – 3, 205 – 224 (2013) / **DOI** 10.1002/prop.201200068

Exceptional and diabolical points in stability questions

Oleg N. Kirillov*

Helmholtz-Zentrum Dresden-Rossendorf, POB 51 01 19, 01314 Dresden, Germany

Received 31 March 2012, revised 25 April 2012, accepted 2 May 2012
Published online 6 June 2012

Key words Non-Hermitian Hamiltonian, exceptional point, stability, non-conservative system.

"I never satisfy myself until I can make a mechanical model of a thing" - guided by this motto of Lord Kelvin we would like to invite a reader to look at some modern concepts such as a non-Hermitian Hamiltonian, exceptional points, the geometric phase, and $\mathcal{PT}$-symmetry, through the prism of the classical mechanics and stability theory. Mathematical and historical parallels discussed in the paper evidence that positions occupied by the non-Hermitian physics and non-conservative mechanics are closer to each other than one might expect.

1 Introduction

W. Thomson (Lord Kelvin) once admitted: "I never satisfy myself until I can make a mechanical model of a thing. If I can make a mechanical model, I understand it. As long as I cannot make a mechanical model all the way through I cannot understand" [1]. Recent years have seen a tremendous activity related to the non-Hermitian Hamiltonians in physics and, in particular, to the *physics of non-Hermitian degeneracies* – so called diabolical and exceptional points [2–5]. In mechanics, these spectral singularities correspond to the semi-simple and non-semisimple $1:1$ resonances that in many cases determine peculiar stability properties of a mechanical system. This short survey should be seen as a brief introduction to the labyrinth of *mechanics of diabolical and exceptional points*. Let a simple but paradigmatic model of the Brouwer's rotating saddle trap serve us as an Ariadne's thread in this adventure.

2 Gyroscopic stabilization on a rotating surface

In 1918 Luitzen Egbertus (Bertus) Jan Brouwer (1881–1966) – a founder of modern topology who established, for example, the topological invariance of dimension and the fixpoint theorem – considered stability of equilibrium of a heavy particle in a rotating vessel [6, 7] [1].

2.1 Brouwer's mechanical model

Let us imagine a particle of unit mass moving on a surface that has a horizontal tangent plane at some point O and rotates with a constant angular velocity Ω around a vertical axis through O in a counter-clockwise direction, Fig. 1.

In the co-rotating frame (x, y, z) with the origin at O and the (x, z)- and (y, z)-plane of which coincide with the principal normal sections of the surface at O, in the assumption that the particle moves without

* E-mail: o.kirillov@hzdr.de, Phone: +49 351 260 2154

[1] Curiously enough, in 1917 motivated by meteorological applications Francis John Welsh Whipple (1876–1943) studied a not unrelated problem on the motion of a particle on the surface of a rotating globe [8].

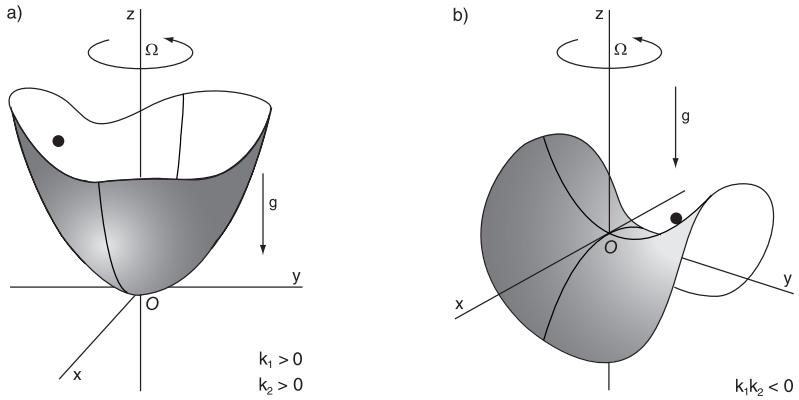

Fig. 1 Brouwer's particle on a rotating (a) cavity and (b) saddle [32].

friction, the equations of motion linearized about the equilibrium position O, have the form [7]

$$\ddot{x} - 2\Omega\dot{y} + \left(k_1 - \Omega^2\right) x = 0, \quad \ddot{y} + 2\Omega\dot{x} + \left(k_2 - \Omega^2\right) y = 0, \tag{1}$$

where dot indicates time differentiation, $k_{1,2} = g/r_{1,2}$, g is the gravity acceleration, and $r_1$and r_2 are the radii of curvature of the intersection of the surface with the (x, z)- and (y, z)-plane, respectively, $r_1 \neq r_2$.

2.2 Eigenvalue problem and characteristic equation

Assuming solution of the linear system of differential equations (1) in the form $x = X\exp(\lambda t)$ and $y = Y\exp(\lambda t)$, we arrive at the homogeneous system of algebraic equations with respect to X and Y

$$\mathbf{L}\mathbf{u} = 0, \quad \mathbf{L}(\lambda) = \mathbf{I}\lambda^2 + 2\Omega\mathbf{J}\lambda + \mathbf{K} + (\Omega\mathbf{J})^2, \tag{2}$$

where

$$\mathbf{u} = \begin{pmatrix} X \\ Y \end{pmatrix}, \quad \mathbf{I} = \begin{pmatrix} 1 & 0 \\ 0 & 1 \end{pmatrix}, \quad \mathbf{J} = \begin{pmatrix} 0 & -1 \\ 1 & 0 \end{pmatrix}, \quad \mathbf{K} = \begin{pmatrix} k_1 & 0 \\ 0 & k_2 \end{pmatrix}. \tag{3}$$

Eq. (2) is one of the standard forms of eigenvalue problems associated with gyroscopic systems [9, 10]. It has a non-trivial solution if and only if $\det\left(\mathbf{L}(\lambda)\right) = 0$, which results in the characteristic equation for λ

$$a_0\lambda^4 + a_1\lambda^2 + a_2 = 0, \quad a_0 = 1, \quad a_1 = k_1 + k_2 + 2\Omega^2, \quad a_2 = (k_1 - \Omega^2)(k_2 - \Omega^2). \tag{4}$$

The roots of the Eq. (4) are eigenvalues of the eigenvalue problem (2). Together with the eigenvectors $\mathbf{u}$ that are the corresponding solutions of Eq. (2) and the generalized eigenvectors that will be introduced in the following, they determine time evolution of the solutions of the linear system (1).

Biquadratic equation (4) can be solved exactly

$$\lambda^2 = -\frac{k_1 + k_2 + 2\Omega^2}{2} \pm \frac{1}{2}\sqrt{(k_1 - k_2)^2 + 8\Omega^2(k_1 + k_2)}. \tag{5}$$

A necessary and sufficient condition for all λ^2s to be real is that the discriminant of the polynomial (the radicand in (5)) is non-negative [11, 12]

$$D := (k_1 - k_2)^2 + 8\Omega^2(k_1 + k_2) \geq 0. \tag{6}$$

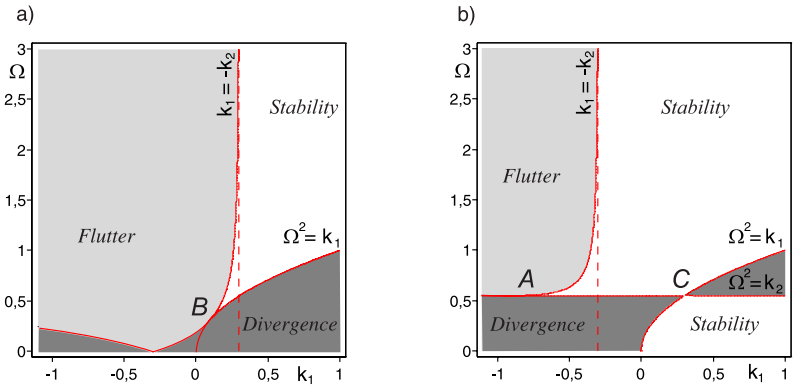

Fig. 2 (online colour at: www.fp-journal.org) Stability diagram of the Brouwer's problem in the (k_1, Ω) plane for (a) $k_2 = -0.3$ and (b) $k_2 = 0.3$.

Moreover, the real λ^2s are all non-positive if and only if $a_1 \geq 0$ and $a_2 \geq 0$, which after taking into account expressions (4), yields

$$k_1 + k_2 + 2\Omega^2 \geq 0, \quad (k_1 - \Omega^2)(k_2 - \Omega^2) \geq 0. \tag{7}$$

Inequalities (6) and (7) form a criterion for the eigenvalues λ to be all pure imaginary, i.e. $\lambda = \pm i\omega$, where $\omega \geq 0$ is real (*spectral stability*). This is however only a necessary condition for all the solutions to the linear equation (1) to be bounded and thus to be *marginally (linearly) stable* [13].

2.3 Eigencurves and bifurcation of multiple eigenvalues

Among the pure imaginary or zero eigenvalues may occur repeated roots of the characteristic equation (4). Indeed, according to Eq. (5), the eigenvalues are double in the discriminant set $D = 0$ being pure imaginary when $a_1 \neq 0$ and zero when $a_1 = 0$. This set bounds the light grey domains in (k_1, Ω) plane in Fig. 2 while the set $a_2 = 0$ corresponds to the double eigenvalues $\lambda = 0$ and bounds the dark grey domains. The eigenvalues that are repeated roots of the characteristic equation are said to have an *algebraic multiplicity* [14, 15].

Evolution of eigenvalues when the white and grey domains in Fig. 2 are crossed with the variation of parameters, is presented as *eigencurves* [16] in the $(\mathrm{Re}\lambda, \mathrm{Im}\lambda, \Omega)$ space in Fig. 3. When $k_1 = 0.25$

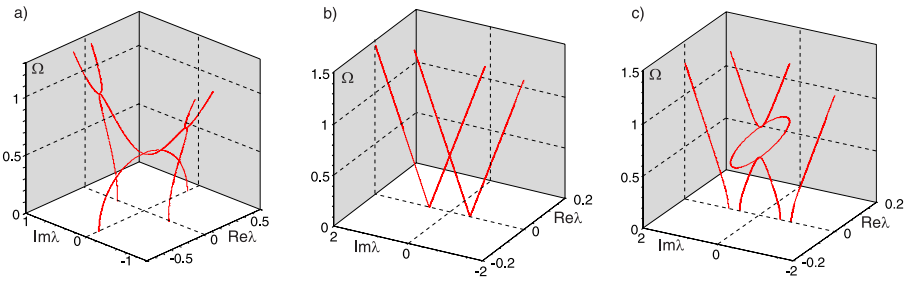

Fig. 3 (online colour at: www.fp-journal.org) Evolution of eigenvalues with the variation of the rotation speed for (a) a saddle with $k_1 = 0.25$ and $k_2 = -0.3$ (gyroscopic stabilization), (b) symmetric concave surface with $k_1 = k_2 = 0.3$ (Campbell diagram), and (c) non-symmetric concave surface with $k_1 = 0.7$ and $k_2 = 0.3$ (bubble of instability and avoided crossings).

and $k_2 = -0.3$ the surface is a saddle and the equilibrium of the Brouwer's particle is unstable without rotation. Indeed, when $\Omega = 0$, there exist a complex-conjugate pair of pure imaginary eigenvalues and two real ones of different signs, Fig. 3(a). A positive real eigenvalue corresponds to an exponentially growing non-oscillatory solution which is known as *divergence* or *static instability* [17], see Fig. 4(a).

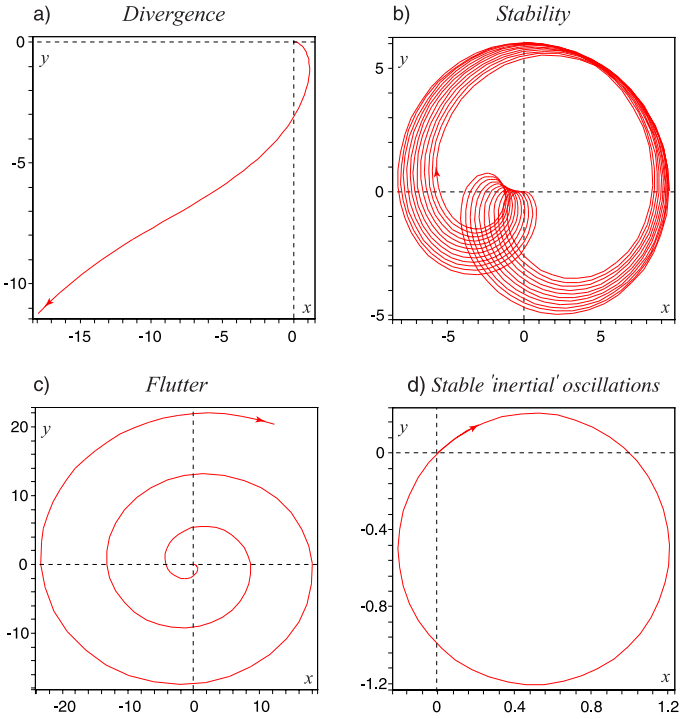

Fig. 4 (online colour at: www.fp-journal.org) Trajectories of the Brouwer's particle in (x, y) plane when $k_1 = 0.25$, $k_2 = -0.3$, $x(0) = 0$, $\dot{x} = 1$, $y(0) = 0$ and $\dot{y}(0) = 0$: (a) escaping by divergence at $\Omega = 0.4$ when $0 \le t \le 8$, (b) trapping at $\Omega = 0.6$ when $0 \le t \le 200$, (c) escaping by flutter at $\Omega = 0.9$ when $0 \le t \le 20$. (d) Stable inertial oscillations at the point C with $k_1 = k_2 = 1$ and $\Omega = 1$ when $x(0) = 0$, $\dot{x}(0) = 1$, $y(0) = 0$, $\dot{y}(0) = 1$ and $0 \le t \le \pi$.

With the increasing angular velocity, the magnitude of the real eigenvalues becomes smaller until they collide at the origin and form a zero eigenvalue of algebraic multiplicity 2. If Ω grows further, the double eigenvalue splits into two pure imaginary eigenvalues, Fig. 3(a). Then all the eigenvalues are pure imaginary of algebraic multiplicity 1 (i.e. *simple*) and the equilibrium is marginally stable.

Therefore, a sufficiently fast rotation of a saddle results in the *gyroscopic stabilization* [18] or *trapping* [19] of the particle, Fig. 4(b). The curve $a_2 = 0$, corresponding to double zero eigenvalues, forms a boundary between the domains of divergence (dark grey) and stability (white), Fig. 2(a).

What are the eigenvectors at the double zero eigenvalues? On the curve $k_1 = \Omega^2$ when $\Omega^2 \neq k_2$ every eigenvector is of the form $\mathbf{u}_0^T = C_1(1, 0)$, where C_1 is an arbitrary constant. Any two such vectors are linearly dependent. The number of linearly independent eigenvectors at the eigenvalue is its *geometric multiplicity*. Thus, at the points of the boundary $k_1 = \Omega^2$ when $\Omega^2 \neq k_2$, zero eigenvalues have algebraic multiplicity 2 and geometric multiplicity 1 and the *defect*, i.e. the difference between the multiplicities, equal to one [14, 15].

Nevertheless, such a *defective eigenvalue* possesses another vector, $\mathbf{u}_1^T = (C_2, 2\Omega C_1/(\Omega^2 - k_2))$, that satisfies a non-homogeneous equation [20]

$$\mathbf{L}\mathbf{u}_1 + \frac{\partial \mathbf{L}}{\partial \lambda}\mathbf{u}_0\bigg|_{\lambda=0} = 0. \tag{8}$$

The eigenvector $\mathbf{u}_0$ and the *generalized eigenvector* $\mathbf{u}_1$ constitute what is known as the *Keldysh chain* in the theory of matrix polynomials [20, 21] and the *Jordan chain* in the matrix theory [22]. The solution, corresponding to a double eigenvalue with the defect 1, involves the both vectors of the chain

$$\mathbf{z}(t) = (\mathbf{u}_1 + \mathbf{u}_0 t)e^{\lambda t}, \tag{9}$$

where $\mathbf{z}^T = (x, y)$. The linear in t *secular term* makes the solution (9) growing even if λ is vanishing or pure imaginary, in contrast to the case of a simple eigenvalue when $\mathbf{z}(t) = \mathbf{u}_0 e^{\lambda t}$. Therefore, despite at the line $a_2 = 0$ separating the stability and divergence domains, double eigenvalues are zero, the corresponding solutions are still statically unstable with the linear growth in time when a doublet has the Keldysh chain. The growth is exponential at the inner points of the dark grey divergence domain in Fig. 2.

The gyroscopically trapped Brouwer's particle can escape the *rotating saddle trap* when $k_1 < -k_2$ and the speed Ω is high enough, Fig. 2(a). Approaching the upper bound for Ω, two pure imaginary eigenvalues merge into a double one with the defect 1. When Ω comes inside the light grey domain in Fig. 2(a), the double eigenvalue splits into two complex eigenvalues, one of them with $\mathrm{Re}\lambda > 0$, Fig. 3(a). This eigenvalue corresponds to an oscillatory solution with the exponentially growing amplitude (*flutter*), see Fig. 4(c). At the flutter boundary the amplitude of the oscillatory solution is growing linearly in time owing to the secular term. This scenario of transition from stability to flutter is known as the *Krein collision* [23, 24] or the *Hamiltonian-Hopf bifurcation* [25].

The stability gap between the flutter and divergence domains, decreases when the parameter $k_1 > 0$ approaches the point B in Fig. 2(a). At this point the boundaries of the two instability domains touch each other, forming a cuspidal singularity. At the *cuspidal point* there exists a defective zero eigenvalue of algebraic multiplicity 4 and geometric multiplicity 1. The same singularity occurs for $k_1 < 0$ and $k_2 > 0$ at the point A in Fig. 2(b). At the singular points the equilibrium is unstable because of secular terms.

At the singular point C in Fig. 2(b) the divergence boundaries $k_1 = \Omega^2$ and $k_2 = \Omega^2$ intersect each other. The curvatures k_1 and k_2 are equal at this self-intersection. When they are non-vanishing, there exist a pair of pure imaginary eigenvalues and a double zero one at C. In this symmetric case the eigenvalues as functions of Ω remain pure imaginary in the vicinity of the zero doublet, see Fig. 3(b). For $k_1 = k_2 > 0$ the eigenvalues are *passing* [26] through each other at zero when Ω is varying without *splitting*, see Fig. 3(b). The latter however is typical at any other point of the divergence boundary, Fig. 3(a,c).

The rotating symmetric concave cup does not have a preferable less steep direction that could provoke the Brouwer's particle to escape. Indeed, the solution corresponding to the double zero eigenvalue is free from secular terms. This happens because there are two linearly independent eigenvectors at the double eigenvalue, which is a *semi-simple eigenvalue* [15] with algebraic and geometric multiplicity 2. The point C in Fig. 2(b) thus belongs to the stability domain.

Since at C the gravitational and centrifugal forces are in balance, the sole Coriolis force causes the Brouwer's particle to rotate along an eccentric circle with the frequency 2Ω, see Fig. 4(d). In geophysics such a motion is known as *inertial oscillations* or *inertial waves* that would occur in the atmosphere or in the ocean in case if the Coriolis force would not have a dependence on the latitude (the β-effect), see e.g. [27, 28].

When $k_1 = k_2 = 0$, which happens when either the gravity is absent or the surface is flat, the point C is at the origin in the (k_1, k_2, Ω) space. However, the equilibrium of the particle on the flat non-rotating surface is unstable: any perturbation in its velocity yields a linear in time increase in the coordinate. These secular terms correspond to two double zero eigenvalues, each of geometric multiplicity 1, which was suggested by the physical reasoning, a bit in the spirit of the insightful book by Mark Levi [29].

Indeed, at $\Omega = 0$ and $k_1 = k_2 = 0$ Brouwer's equations (1) decouple. With the new variables $x_1 = x$, $x_2 = \dot{x}$ and $y_1 = y$, $y_2 = \dot{y}$, the equations $\ddot{x} = 0$ and $\ddot{y} = 0$ take the form $\dot{\mathbf{q}} = \mathbf{A}\mathbf{q}$, where $\mathbf{q}^T = (x_1, x_2, y_1, y_2)$, and

$$\mathbf{A} = \begin{pmatrix} 0 & 1 & 0 & 0 \\ 0 & 0 & 0 & 0 \\ 0 & 0 & 0 & 1 \\ 0 & 0 & 0 & 0 \end{pmatrix}.$$

The matrix $\mathbf{A}$ contains a pair of Jordan blocks with double zero eigenvalues ($0^2 0^2$ in notation proposed by Arnold [30]). Assuming $k_2 = \kappa k_1$ in Eq. (1) we find that the two double eigenvalues at $\Omega = 0$ split as $\lambda_{1,2} = \pm i\sqrt{k_1}$ and $\lambda_{3,4} = \pm i\sqrt{\kappa k_1}$, see Fig. 5(a). This type of splitting was observed in the spectrum of the Couette-Taylor flow and of the Bose-Hubbard model, see [31] and references therein. At $\Omega \neq 0$, the degeneracy is removed and the eigencurves develop a bubble of (divergence) instability, Fig. 5(b).

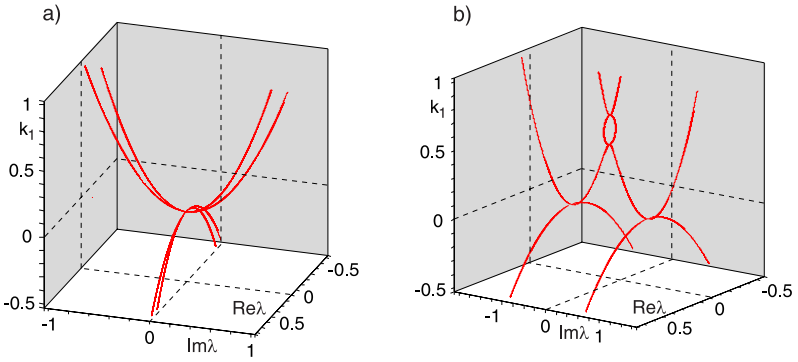

Fig. 5 (online colour at: www.fp-journal.org) Evolution of eigenvalues with the variation of k_1 in the $(\mathrm{Re}\lambda, \mathrm{Im}\lambda, k_1)$ space when $k_2 = \kappa k_1$ and $\kappa = 0.7$ at (a) $\Omega = 0$ and (b) $\Omega = 0.7$.

2.4 Singular stability boundary of the rotating saddle trap

The analysis of eigenvalues and eigenvectors performed above suggests the necessary and sufficient conditions for marginal stability of the linear system (1)

$$D > 0, \quad a_2 > 0, \quad k_1 = k_2 = \Omega^2 \; \forall \; \Omega \neq 0. \tag{10}$$

In the (k_1, k_2, Ω) space the stability domain thus consists of the two parts joined along the line SC that lies in the plane $k_1 = k_2$. The boundary of the first part has a form of a trihedral spike with the cuspidal edges SA and SB that project into the lines $k_2 = -3k_1$ and $k_1 = -3k_2$ in the (k_1, k_2)-plane shown by red dashed lines in Fig. 6 and the transversal intersection SC that touch each other at the origin. The boundary of another part has only a dihedral angle singularity along SC. The system is stable at the inner points of the domains as well as on the edge SC when $\Omega \neq 0$.

The trihedral spike corresponds to the stability for large angular velocities according to Brouwer's classification. Indeed, both the stability region in Fig. 2(a) and the upper stability region in Fig. 2(b) are slices of it. In Brouwer's interpretation 'as long as in O the principal curvature, concave in an upward direction, is less than three times the one concave in a downward direction, there are rotation velocities for which the motion of the particle on the rotating saddle yields formal stability' [7].

This challenging the common sense conclusion of Brouwer follows from the proportions of the cross-section of the spike by the $\Omega = \mathrm{const}$ plane that has a form of a curvilinear triangle ABC, Fig. 6(b).

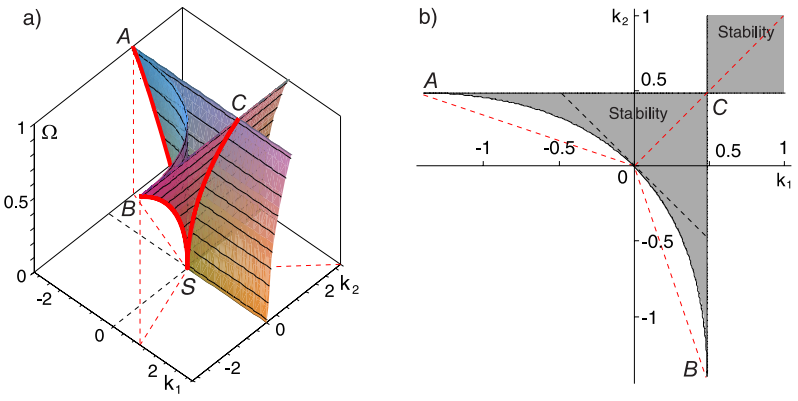

Fig. 6 (online colour at: www.fp-journal.org) (a) Stability boundary of the Brouwer's problem with the Swallowtail-like singularity at the origin in the (k_1, k_2, Ω) space and (b) the domain of marginal stability in the (k_1, k_2) plane for $\Omega = 0.7$ with the red dashed lines indicating projections of the two cuspidal edges SA and SB and the line of self-intersection SC [32].

Similar planar stability domains were observed in numerous problems of gyroscopic stabilization, e.g. for a mass mounted on a non-circular weightless rotating shaft subject to a constant axial compression force [10, 33, 34] or in a recent study of levitation of a rotating body carrying a point electrical charge in the field of a fixed point charge of the same sign [35].

A beautiful connection exists between the boundaries of the domain of the gyroscopic stabilization and the eigenvalues $\sigma_{1,2}(\mathbf{K})$ of the matrix $\mathbf{K}$ of potential forces and those of the rotationally symmetric matrix

$$\mathbf{K}_A = (\mathbf{K} - \mathbf{JKJ})/2 = \mathbf{I}(k_1 + k_2)/2, \tag{11}$$

representing a sort of 'averaged' $\mathbf{K}$ around the rotation axis [36].

Already in Fig. 2(b) it is visible that the lower bound of the region of gyroscopic stabilization at large angular velocities is determined by $\sigma_{1,2}(\mathbf{K})$ as $\Omega_d^2 = \max(\sigma_1(\mathbf{K}), \sigma_2(\mathbf{K}))$. According to Veselić [36], $\mathbf{K}_A > 0$ is a necessary and sufficient condition for the absence of the upper bound on the gyroscopic parameter Ω. Hence, the gyroscopically stabilized Brouwer's particle will not escape the trap with the arbitrary increase of $|\Omega| > |\Omega_d|$ if and only if $k_1 + k_2 > 0$. This condition defines the vertical asymptotes to the flutter domain in Fig. 2. Hence, at low rotation speeds of a saddle, it is negative eigenvalues of $\mathbf{K}_A$ that determine the existence of the upper bound for the gyroscopic stabilization, which is necessary for the origination of the cuspidal singularities on the stability boundary [36].

The triangle ABC in Fig. 6(b) is connected at the corner C to the domain of stability for small angular velocities given by the inequalities $k_1 > \Omega^2$ and $k_2 > \Omega^2$ (cf. the lower stability region in Fig. 2(b)). This part of the stability diagram was found already in 1869 by Rankine[2] [37] whereas the triangle ABC was reconstructed by joint efforts of Föppl[3] (1895) [38], von Kármán[4] (1910) [39], Prandtl[5] (1918) [40], Brouwer (1918) [7], and Jeffcott[6] (1919) [41].

[2] William John Macquorn Rankine (1820-1872) – a Scottish engineer and physicist, an author e. g. of the Rankine vortex model and Rankine-Hugoniot conditions in gas dynamics and at the same time of one of the first studies on stability of bicycles.

[3] August Otto Föppl (1854-1924) – a German civil engineer, a student of C. Mohr and an advisor of L. Prandtl; well known are e. g. the Föppl-von Kármán equations for large deflections of thin flat plates.

[4] Theodore von Kármán (1881–1963) – a Hungarian-German-American aerospace engineer and fluid dynamist, one of the founders of the Jet Propulsion Laboratory.

[5] Ludwig Prandtl (1875–1953) – a German scientist, one of the creators of aerodynamics.

[6] Henry Homan Jeffcott (1877–1937) – an Irish engineer developed the *Jeffcott rotor* model.

The *Swallowtail*-like surface bounding the stability domain of the Brouwer's heavy particle in a rotating vessel, perfectly symbolizes the variety of applications to which this mechanical model is connected. Almost literally at every corner of the surface shown in Fig. 6(a) lives a physical phenomenon.

3 Manifestations of Brouwer's model in physics

3.1 Stability of deformable rotors

With the equal positive coefficients $k_1 = k_2 > 0$, the Brouwer's equations (1) coincide with that of the idealized model of the classical rotor dynamics problem of shaft whirl by Föppl [38], von Kármán [39], and Jeffcott [41], written in the rotating (x, y)-frame.

Indeed, a deformable shaft carrying, e.g., a turbine wheel, and rotating with the angular speed Ω about its axis of symmetry can be modeled as a planar oscillator on a rotating plate [42], i.e. as a unit mass point that is suspended symmetrically by massless springs with the effective stiffness coefficients $k_1 = k_2 = k$ from the frame that rotates with the angular velocity Ω [43,44], see Fig. 7(a). On the other hand, this model arises in the theory of modern micro-mechanical Coriolis vibratory gyroscopes (CVG) [45].

For the stationary $(\Omega = 0)$ symmetrical Föppl-von Kármán-Jeffcott rotor the transverse bending modes occur in pairs with equal natural frequencies $\omega = \sqrt{k}$ for vibrations in orthogonal diametral planes. When the vibrations of such a pair are combined with equal amplitudes and a quarter period phase difference, the result is a *circularly polarized* vibration – a clockwise- or a counter-clockwise circular *whirling* motion with the whirl rate $\omega > 0$ [43, 44]. This phenomenon is related to the *Doppler splitting* of the doublet modes into the forward and backward traveling waves propagating along the circumferential direction of a rotating elastic solid of revolution, known already to Bryan[7] in 1890 [46–48].

According to the Brouwer's stability conditions (10), the symmetrical Föppl-von Kármán-Jeffcott rotor is marginally stable at any speed Ω. Indeed, the part of the plane $k_1 = k_2$ corresponding to $k_{1,2} > 0$ belongs to the domain of marginal stability, as is seen in the stability diagrams of Fig. 6.

The symmetry of the Föppl-von Kármán-Jeffcott rotor is, however, a latent source of its instability. Destabilization can be caused already by constraining the mass point to vibrate along a rotating diameter. For example, if a guide rail is installed along the x-axis so that y is constrained to vanish identically, equation (1) reduces to the 1869 model by Rankine [37]: $\ddot{x} + (k_1 - \Omega^2)x = 0$, which predicts unbounded growth for x as soon as $\Omega^2 > k_1$, i.e. as soon as the centrifugal field overpowers the elastic field [43, 44]. In the diagram of Fig. 6(b) Rankine's instability threshold (critical rotating speed) bounds the infinite stability domain with the corner at the point C showing that the constraint could also be achieved by tending one of the stiffness coefficients to infinity. Note that recently Baillieul and Levi motivated by stabilization of satellites with flexible parts, studied the dynamical effects of imposing constraints on the relative motions of component parts in a rotating mechanical system or structure and in particular in the Brouwer's equations [49].

After successful demonstration by De Laval[8] in 1889 of a well-balanced gas turbine running stably at supercritical, i.e. unstable by Rankine, speeds Ω, the model of Rankine [37] has been recognized as inadequate [43, 44]. Nevertheless, its instability threshold is just a part of the singular stability boundary of the Brouwer's equations shown in Fig. 6.

---

[7] George Hartley Bryan (1864–1928) – a British physicist, discoverer of the *wave inertia effect* (Bryan's effect) in rotating shells and originator of the equations of airplane motion.

[8] Karl Gustaf Patrik de Laval (1845–1913) – a Swedish engineer and inventor, founder of the Alpha Laval Company. Rankine's pessimistic predictions of instabilities at high speeds were widely accepted among engineers and discouraged the development of high speed rotors until the De Laval's invention of 1889. Being inspired by De Laval's success, Föppl proposed in 1895 a model that is now known as the Jeffcott rotor [38]. In 1916 another experimental evidence of a rotor operating stably above the Rankine's threshold was published by Kerr [50]. This publication motivated the Royal Society of London to commission Jeffcott to resolve the conflict between Rankine's theory and the practice of Kerr and De Laval [51]. Jeffcott's work came out of print in 1919 [41].

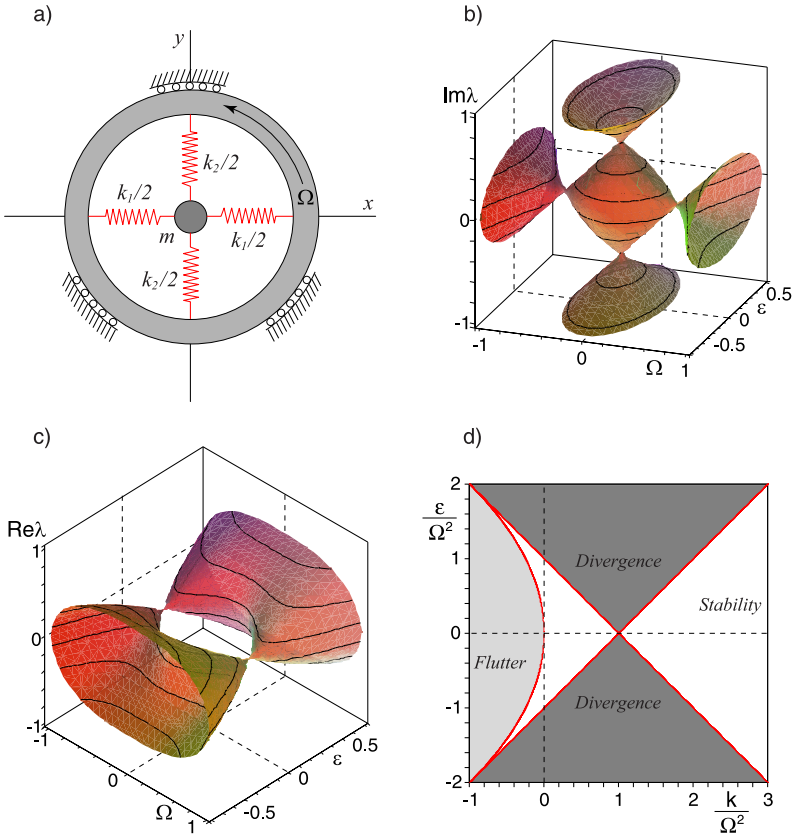

Fig. 7 (online colour at: www.fp-journal.org) (a) A Prandtl-Smith model of whirling shaft [43,44]: A point mass $m = 1$ suspended by the springs from the frame that rotates with the angular velocity Ω. (b) Whirling frequencies of the Prandtl-Smith rotor with $k_1 = k + \varepsilon$, $k_2 = k - \varepsilon$, and $k = 0.3$ as a function of Ω and ε form a singular surface with four conical points in the plane $\varepsilon = 0$. (c) Growth rates of the Prandtl-Smith rotor showing instability due to stiffness detuning near the critical speeds $\Omega = \pm\sqrt{k}$. (d) The corresponding stability diagram in the $(\varepsilon\Omega^{-2}, k\Omega^{-2})$ plane given by the conditions (14) and (15). The parameter $k\Omega^{-2}$ has a meaning of the squared *Rossby number* $\mathrm{Ro} = k^{1/2}\Omega^{-1}$ that is adopted in geophysics as a measure of the relative strength of the Coriolis force.

Soon after the success of the symmetric Föppl-von Kármán-Jeffcott model of De Laval's rotor, in 1918 Prandtl [40] noted that if the elastic or inertia properties of a rotor are not symmetric about the axis of rotation there may be speed ranges where the rotor whirl is unstable. He pointed out the analogy between a rotor whose shaft had unequal principal stiffness coefficients $(k_1 \neq k_2)$ and a pendulum mounted asymmetrically on a turntable[9]. The pendulum was unstable when the turntable rotation rate Ω was between the pendulum natural frequencies in the soft and stiff directions [43, 44]. Similar instability due to inertia asymmetry was discussed by Smith[10] in 1933 [52]. For positive coefficients $k_1 \neq k_2$, the Brouwer's equations (1) constitute exactly the undamped model by Prandtl and Smith, Fig. 7(a).

[9] When $k_1 = k_2 > 0$ and the 'turntable' is the Earth, the Brouwer's equations describe small oscillations of the *Foucault pendulum* [56].

[10] David MacLeish Smith (1900–1986) – a Scottish engineer participated in the development of the first British axial flow jet engine for aircraft.

Assume in Eq. (1) that $k_1 = k + \varepsilon$ and $k_2 = k - \varepsilon$ [43, 44]. Calculating imaginary parts of the roots of the equation (4) we find the implicit equation for the whirling frequencies in the Prandtl-Smith model

$$((\mathrm{Im}\lambda)^2 - k - \Omega^2)^2 - 4\Omega^2 k = \varepsilon^2. \tag{12}$$

In the $(\Omega, \varepsilon, \mathrm{Im}\lambda)$ space the whirling frequencies form a singular surface with four conical points, Fig. 7(b). The slice of this surface by the plane $\varepsilon = 0$ shows four straight lines intersecting each other at the conical points at $\Omega = 0$ and at the critical speeds $\Omega = \pm\sqrt{k}$, see Fig. 3(b). These eigencurves constitute the *Campbell* [11] *diagram* [53] of the ideal Föppl-von Kármán-Jeffcott rotor.

Stiffness modification with the variation of ε corresponds to the eigencurves in a slice of the eigenvalue surface by the plane that departs of the conical singularities by a distance $\varepsilon \neq 0$. In the vicinity of $\Omega = 0$ the eigencurves demonstrate *avoided crossings* or *veering* while near the critical speeds $\Omega = \pm\sqrt{k}$ the eigenvalues are real with zero frequency, Fig. 3(c). As Fig. 7(c) shows, the real eigenvalues (growth rates) lie on a singular eigenvalue surface with two conical points at the critical speeds

$$((\mathrm{Re}\lambda)^2 + k + \Omega^2)^2 - 4\Omega^2 k = \varepsilon^2. \tag{13}$$

The slices of the surface (13) by the planes $\varepsilon \neq 0$ in the vicinity of the apexes of the cones are closed loops named *bubbles of instability* by MacKay in 1986 [13], see Fig. 3(c). Hence, for $\varepsilon \neq 0$, the Prandtl-Smith rotor is unstable by divergence at the speeds in the interval

$$\sqrt{k - \varepsilon} < |\Omega| < \sqrt{k + \varepsilon}, \tag{14}$$

provided that

$$\varepsilon^2 + 4\Omega^2 k > 0. \tag{15}$$

The stability diagram in the $(\varepsilon\Omega^{-2}, k\Omega^{-2})$ plane corresponding to the inequalities (14) and (15) is actually a rotated by an angle $\frac{\pi}{4}$ diagram given by the conditions (10), cf. Fig. 6(b) and Fig. 7(d). In this orientation Brouwer's stability diagram frequently appears also in *accelerator physics*, see e.g. [54, 55].

The amount of kinetic energy available in the rotor is usually orders of magnitude greater than the deformational energy which any internal mode can absorb. Therefore, already small deviations from the ideal conditions yield coupling between modes that by transferring even a tiny fraction of the rotational energy can initiate failure in the vibratory mode [43, 44].

The conical singularities on the surfaces of frequencies and growth rates arise as a result of unfolding of double semi-simple eigenvalues of the Föppl-von Kármán-Jeffcott rotor that exist at $\Omega = 0$ ($\lambda = \pm i\omega$) and at the critical speeds $\Omega = \pm\sqrt{k}$ ($\lambda = 0$), where $i = \sqrt{-1}$. The doublets originate at the crossings of the branches of the Campbell diagram corresponding to $\varepsilon = 0$, Fig. 3(b),

$$\lambda_p^+ = i\omega + i\Omega, \quad \lambda_n^+ = i\omega - i\Omega, \quad \lambda_p^- = -i\omega + i\Omega, \quad \lambda_n^- = -i\omega - i\Omega. \tag{16}$$

The eigenvectors at the eigenvalues (16) are

$$\mathbf{u}_p^+ = \begin{pmatrix} -i \\ 1 \end{pmatrix}, \quad \mathbf{u}_n^+ = \begin{pmatrix} i \\ 1 \end{pmatrix}, \quad \mathbf{u}_p^- = \begin{pmatrix} -i \\ 1 \end{pmatrix}, \quad \mathbf{u}_n^- = \begin{pmatrix} i \\ 1 \end{pmatrix}. \tag{17}$$

The eigenvalue problem (2) can be rewritten in the form $\mathbf{A}\mathbf{a} = \lambda\mathbf{a}$ with the Hamiltonian matrix $\mathbf{A}$ and the vector $\mathbf{a}$ defined as

$$\mathbf{A} = \begin{pmatrix} -\Omega\mathbf{J} & \mathbf{I} \\ -\mathbf{K} & -\Omega\mathbf{J} \end{pmatrix} = \mathbf{S}\mathbf{A}^T\mathbf{S}, \ \mathbf{S} = \begin{pmatrix} 0 & -\mathbf{I} \\ \mathbf{I} & 0 \end{pmatrix}, \ \mathbf{a} = \begin{pmatrix} \mathbf{u} \\ \lambda\mathbf{u} + \Omega\mathbf{J}\mathbf{u} \end{pmatrix}. \tag{18}$$

[11] Wilfred Campbell (1884–1924) – an engineer at General Electric Company who first proposed the frequency-rotation speed diagram for predicting the critical speeds of rotors.

For every eigenvalue in (16), the sign of the quantity $i\overline{\mathbf{a}}^T\mathbf{S}\mathbf{a}$, where overbar denotes complex conjugate and $\mathbf{a}$ is constructed by means of the corresponding eigenvectors of (17), defines its *symplectic* or *Krein signature* [13, 58]. The eigenvalues λ_p^+ and λ_n^+ branching from the doublet $i\omega$ have the positive signature while for λ_p^- and λ_n^- that branch from $-i\omega$, it is negative. Indeed,

$$i\overline{\mathbf{a}_p^+}^T\mathbf{S}\mathbf{a}_p^+ = 4\omega,\ i\overline{\mathbf{a}_n^+}^T\mathbf{S}\mathbf{a}_n^+ = 4\omega,\ i\overline{\mathbf{a}_p^-}^T\mathbf{S}\mathbf{a}_p^- = -4\omega,\ i\overline{\mathbf{a}_n^-}^T\mathbf{S}\mathbf{a}_n^- = -4\omega. \tag{19}$$

In 1986, MacKay [13] studied unfoldings of the semi-simple double pure imaginary and zero eigenvalues in general Hamiltonian systems and demonstrated that the orientation of the cones depends on the Krein signature [24] of the doublets. At $\Omega = 0$ the doublets at the crossing of the branches λ_p^+ and λ_n^+ have definite Krein signature. Then according to MacKay the frequency cones are oriented vertically in the $(\Omega, \varepsilon, \mathrm{Im}\lambda)$-space that yields avoided crossings in their slices and thus stability, see Fig. 7(b). If the doublet has a mixed Krein signature, as it happens at the crossing of the branches λ_n^+ and λ_p^-, there appears a differently oriented eigenvalue cone for the real parts of the perturbed eigenvalues that possesses bubbles of instability in its cross-sections, Fig. 7(c).

Therefore, definiteness of the Krein signature of the doublets at $\Omega = 0$, prohibits their unstable unfolding in the region of low angular velocities by the perturbations such as the stiffness modification that preserve the Hamiltonian structure of the equations of motion of the gyroscopic system (1).

3.2 Foucault's pendulum, Bryan's effect, Coriolis Vibratory Gyroscopes and Hannay-Berry phase

A general solution corresponding to the symmetric Brouwer's cavity with the eigenvalues (16) and eigenvectors (17) is

$$\mathbf{z}(t) = C_1\mathbf{u}_p^+ e^{\lambda_p^+ t} + C_2\mathbf{u}_n^+ e^{\lambda_n^+ t} + C_3\mathbf{u}_p^- e^{\lambda_p^- t} + C_4\mathbf{u}_n^- e^{\lambda_n^- t}. \tag{20}$$

For example, initial conditions $x(0) = y(0) = 0$ and $\dot{x}(0) = \dot{y}(0) = 1$ yield

$$x(t) = (\cos\Omega t + \sin\Omega t)\omega^{-1}\sin\omega t, \quad y(t) = (\cos\Omega t - \sin\Omega t)\omega^{-1}\sin\omega t. \tag{21}$$

In the low speed region when $\Omega \ll \omega$, equations (20) and (21) describe *modulated oscillations* with the modulation frequency Ω and the carrier frequency ω. In the (x, y) plane of the rotating frame the particle traces narrow petals of a rose curve (21) drawing new petals in the clockwise direction, see Fig. 8(a). This means that the swing plane of the particle in the cavity slowly precesses with the angular velocity $\Omega_p = -\Omega$. This angular shift should not be surprising if we remember the Prandtl remark that Brouwer's equations (1) describe small oscillations of a pendulum on a turntable. The symmetric case when $k_1 = k_2$ corresponds to the well-known Foucault[12] pendulum [56, 57].

An effect analogous to the precession of the swing plane of the Foucault pendulum due to the Coriolis force exists in vibrating solids of revolution such as discs, rings, cylinders or shells subjected to a rotation with the speed Ω about the symmetry axis. In 1890 Bryan was the first who observed that the vibrating pattern of standing waves rotates with respect to such a structure at a rate proportional to Ω [46].

Bryan's effect of inertia of standing waves is a working principle of the Coriolis vibratory gyroscopes (CVG) that sense the imposed rotation. A wide variety of designs including micro-electro-mechanical systems (MEMS) have been proposed and built since 1960s [45, 47, 59, 60]. Remarkably, the most of the modern analyses of CVGs are *linear* in nature and view the Coriolis force as providing a coupling between two vibratory modes of the system [59]. For example, a single mass MEMS based CVG without decoupling frame is described by the Brouwer's model (1) and its perturbation [45].

[12] Jean Bernard Léon Foucault (1819–1868) – a French physicist who in 1851 first observed the Bryan's effect caused by the rotation of the Earth and proposed the very term 'gyroscope'.

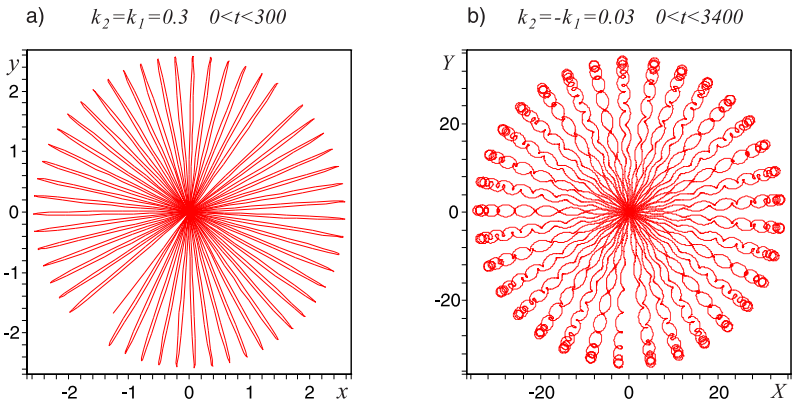

Fig. 8 (online colour at: www.fp-journal.org) (a) A retrograde precession (the *Bryan's effect*) with $\Omega_p = -\Omega$ in the rotating frame (x, y) of the plane of oscillations of the Brouwer's particle in a cavity rotating counter-clockwise with $\Omega = 0.01$ when $x(0) = y(0) = 0$ and $\dot{x}(0) = \dot{y}(0) = 1$; (b) A prograde precession with $\Omega_p = 2k_1^2\Omega$ in the laboratory frame (X, Y) of the orbit of the Brouwer's particle trapped in a saddle rotating with $\Omega = 0.5$ when $X(0) = Y(0) = 0$, $\dot{X}(0) = 0$ and $\dot{Y}(0) = 1$.

In 2003-2004 Andersson and Krishnaprasad [59, 61] demonstrated that the Bryan's effect of imposed slow rotatory motion on a rapidly vibrating structure is geometrical in nature. The angle of the retrograde precession of the nodal points of vibration with respect to the structure itself and hence the precession angle of the orbit of the Brouwer's particle in Fig. 8(a), is exactly the *geometric phase* [62, 63] in the sense of Berry and Hannay [64, 65].

A converse statement came recently from optics where the very *Berry phase* accumulated by a light wave as it propagates along a helical ray in a cylindrical medium was shown to represent the Coriolis effect in a non-inertial coordinate frame accompanying the ray trajectory [66–70]. According to Bliokh 'The Berry phase describes a sort of inertia of the electric field which remains locally non-rotating about the ray' [66]. This observation gives a link to the effect of inertia of the standing wave pattern in vibrating mechanical structures subjected to slow rotation. It should not be surprising then that the Brouwer's model (1) can be encountered with in optics.

3.3 Polarized light within the cholesteric liquid crystal

Indeed, following Marathay [71] let us consider the state of polarization of a plane light wave as it propagates along the helical axis within the nonmagnetic cholesteric liquid crystal. Assume that Z-axis of a right-handed laboratory frame is parallel to the helical axis. The molecular planes of the structure are parallel to the (X, Y)-plane of the laboratory frame. The principal axes of each molecular plane are gradually rotated as one proceeds along Z-direction. Define the pitch p as the minimum distance between the two planes whose principal axes are parallel and introduce the parameter $\Omega = 2\pi/p$. Restricting ourselves by the plane waves that propagate normally to the crystal planes, i.e. along the helical axis, we find from the Maxwell's equations that

$$\partial_Z^2 \mathbf{E} = \frac{\varepsilon(Z)}{c^2}\partial_t^2 \mathbf{E}, \quad \mathbf{E} = \begin{pmatrix} E_X \\ E_Y \end{pmatrix}, \tag{22}$$

where $\mathbf{E} = \mathbf{E}(Z, t)$ is the Jones vector [71]. The 2×2 matrix $\varepsilon(Z)$ describes the dielectric properties of the layer at Z in the laboratory frame and for a right-handed structure in terms of the principal dielectric constants $\varepsilon_{11}^0 > 0$ and $\varepsilon_{22}^0 > 0$ it can be expressed as $\varepsilon(Z) = \mathbf{R}(\Omega Z)\mathbf{T}\mathbf{R}^{-1}(\Omega Z)$, where $\mathbf{T} = \mathrm{diag}\,(\varepsilon_{11}^0, \varepsilon_{22}^0)$

and $\mathbf{R}$ is the rotation matrix

$$\mathbf{R} = \begin{pmatrix} \cos(\Omega Z) & -\sin(\Omega Z) \\ \sin(\Omega Z) & \cos(\Omega Z) \end{pmatrix}. \tag{23}$$

Looking for a time-harmonic solution of Eq. (22) of the form $\mathbf{E}(Z,t) = \mathbf{F}(Z)exp(-i\omega t)$ and transforming to a space-rotating coordinate system by

$$\mathbf{f}(Z) = \mathbf{R}(-\Omega Z)\mathbf{F}(Z), \tag{24}$$

we find that in the space rotating coordinate system (x, y, z) the dynamics of the state of polarization $\mathbf{f}$ is governed by the autonomous equation

$$\ddot{\mathbf{f}} + 2\Omega\mathbf{J}\dot{\mathbf{f}} + (\mu^2\mathbf{T} + (\Omega\mathbf{J})^2)\mathbf{f} = 0, \tag{25}$$

where $\mu^2 = \omega^2/c^2$, the dot stands for the derivative d/dz, and $z = Z$. Equation (25) is the system (1) with $k_1 = \mu^2\varepsilon^0_{11}$ and $k_2 = \mu^2\varepsilon^0_{22}$ corresponding to the Brouwer's particle in a cavity.

A medium with helically varying in space properties, or with *chirality*, can therefore introduce gyroscopic terms in the equations of motion where a spacial variable plays the role of time. In accelerator physics such a chiral environment can be created artificially with the use of the twisted electrostatic [72,73] or magnetic [55, 74] quadrupole lenses as it happens, e.g. in a betatron with stellarator fields [54]. In this case, as will be shown below, equations of the Brouwer's particle on a rotating saddle naturally appear.

3.4 Helical magnetic quadrupole focussing systems

Already in 1914 Brouwer discussed the possibility of experimental verification of stabilization of a heavy ball on a rotating saddle [7]. Nowadays such mechanical demonstrations are available as teaching laboratory experiments [19]. However, the prospects for the first non-trivial physical application of this effect had arisen as early as 1936 when Penning proposed using the quadrupole electric field to confine the charged particles [75].

In the RF-electric-quadrupole *Paul trap* invented in 1953 [76], a saddle-shaped field created to trap a charged ion is not rotating about the ion in the center. The Paul-trap potential can only 'flap' the field up and down, which yields two decoupled Mathieu equations describing the motions of a single ion in the trap. Nevertheless, comparing the rotating saddle trap and the Paul trap, Shapiro [55] and Thompson et al. [19] demonstrated that the former mimics most of the characteristics of the Paul trap such as stability and instability regions, micromotion and secular oscillation frequency [19]. Despite the Brouwer's problem is not only a mechanical analogy to the Paul trap, the equations of the two models are substantially different. Brouwer's system is autonomous, which greatly simplifies its solution. It originates, however, in accelerator physics where it describes strong focussing of the charged particles by a helical magnetic quadrupole lens [54, 77].

Linearized equations of motion in the laboratory (X, Y, Z)-frame of a particle of momentum p and charge e in the helical quadrupole magnetic field rotating with distance along the Z-axis and completing one rotation in an axial distance Λ, in the assumption that $X, Y \ll \Lambda$ are [77]

$$\ddot{X} = -\varepsilon(X\cos Z + Y\sin Z), \quad \ddot{Y} = -\varepsilon(X\sin Z - Y\cos Z), \tag{26}$$

where dot stands for the derivative d/dZ,

$$\varepsilon = \frac{\Lambda^2\nu^2}{16\pi^2}, \quad \nu^2 = \frac{eG}{pc}, \tag{27}$$

and c is the speed of light. The downstream distance Z is measured in units of $\Lambda/(4\pi)$. At $Z = 0$, the components of the magnetic field in the laboratory frame are $B_X = GY$, $B_Y = GX$, $B_Z = 0$ as for the conventional quadrupole.

Changing basis similar to as in the *rotating wave approximation* [19, 78]

$$x = X\cos\frac{Z}{2} + Y\sin\frac{Z}{2}, \quad y = -X\sin\frac{Z}{2} + Y\cos\frac{Z}{2}, \tag{28}$$

transforms periodic equations (26) into the system that is autonomous in the co-moving frame (x, y, z) rotating with the mechanical rotation of the helix

$$\ddot{\mathbf{v}} + \mathbf{J}\dot{\mathbf{v}} + (\mathbf{K} + (\mathbf{J}/2)^2)\mathbf{v} = 0, \tag{29}$$

where dot denotes d/dz, $z = Z$, and

$$\mathbf{v} = \begin{pmatrix} x \\ y \end{pmatrix}, \quad \mathbf{J} = \begin{pmatrix} 0 & -1 \\ 1 & 0 \end{pmatrix}, \quad \mathbf{K} = \begin{pmatrix} \varepsilon & 0 \\ 0 & -\varepsilon \end{pmatrix}. \tag{30}$$

Equations (29), following from (1) when $\Omega = 1/2$ and $k_1 = -k_2 = \varepsilon$, correspond to a rotating saddle. On the stability diagram of the Prandtl-Smith rotor shown in Fig. 7(d) the rotating saddle trap corresponds to the vertical dashed line $k = 0$. The same diagram determines stability of a high current betatron with stellarator field [54]. Since in the laboratory frame the Brouwer's equations (1) transform to that of the two coupled oscillators with periodically varying parameters, such as Eqs. (26), the divergence and flutter domains in the diagram of Fig. 7(d) are often interpreted as the zones of *parametric resonance* [55].

Fig. 7(d) demonstrates that when $|\varepsilon| < \Omega^2$, the quadrupole lens is focussing or the rotating saddle is trapping. When $|\varepsilon| \ll \Omega^2$, the orbit of the particle in the laboratory frame is a fast oscillation of the frequency $2\varepsilon\Omega$ with the imposed micromotions. The average plane of the oscillations experiences a slow prograde precession with the angular velocity $\Omega_p = 2\varepsilon^2\Omega$ [19]. Fig. 8(b) illustrates this precession for $\Omega = 0.5$ and $\varepsilon = -0.03$.

Therefore, if rotational and vibrational time scales are widely separated, the orbit of the Brouwer's particle exhibits similar precession patterns both in a cavity, Fig. 8(a), and on a saddle, Fig. 8(b). Adiabatically slow rotation or vibration yields accumulation of the geometric phase that manifests itself in the particle's orbit precession [59, 79].

3.5 Modulational instability

A monochromatic plane wave with a finite amplitude propagating in a dispersive medium can be disrupted into a train of short pulses when the amplitude exceeds some threshold [80]. This process develops due to an unbounded increase in the percentage modulation of the wave, i.e. instability of the carrier wave with respect to modulations. This is the fundamental for modern fluid dynamics, nonlinear optics and plasma physics *modulational instability* [81, 82].

Without dissipation, a slowly varying in time envelope A of the rapidly oscillating carrier wave is often described by the nonlinear Schrödinger equation

$$iA_t + \alpha A_{xx} + \gamma|A|^2 A = 0. \tag{31}$$

In the equation (31), α and γ are positive real numbers, $i = \sqrt{-1}$, and the modulations are restricted to one space dimension x [83, 84]. The equation (31) has a solution in the form of a monochromatic wave $A = A_0 e^{ikx - i\omega t}$, where the frequency of the modulation, ω, depends on the amplitude $A_0 = u_1^0 + iu_2^0$ and spacial wavenumber k as $\omega = \alpha k^2 - \gamma\|\mathbf{u}_0\|^2$ with $\mathbf{u}_0^T = (u_1^0, u_2^0)$.

Linearizing the nonlinear Schrödinger equation (NLS) about the basic traveling wave solution and assuming periodic in x perturbations with the wavenumber σ we substitute their Fourier expansions into the linearized problem. Then, the stability is determined by the equation

$$\ddot{\mathbf{v}} + 2q\mathbf{J}\dot{\mathbf{v}} + 2\gamma\mathbf{D}\dot{\mathbf{v}} + (\mathbf{P} + (q\mathbf{J})^2)\mathbf{v} = 0, \tag{32}$$

where dot indicates time differentiation, the matrix $\mathbf{J}$ is defined in (30), $q = \alpha\sigma^2 - \gamma\|\mathbf{u}_0\|^2$, $\mathbf{P} = (4\alpha^2k^2\sigma^2 + \gamma^2\|\mathbf{u}_0\|^4)\mathbf{I}$, $\mathbf{D} = \mathbf{u}_0\mathbf{u}_0^T\mathbf{J} - \mathbf{J}\mathbf{u}_0\mathbf{u}_0^T$, and the dyad $\mathbf{u}_0\mathbf{u}_0^T$ is a 2×2 symmetric matrix [32, 83].

Equation (32) is the damped version of the Brouwer's equation (1) with $\Omega = q$ and $k_1 = k_2 = 4\alpha^2k^2\sigma^2 + \gamma^2\|\mathbf{u}_0\|^4$. The 'damping' matrix $\mathbf{D}$ is symmetric and traceless, i.e. it is *indefinite* with the eigenvalues $\mu_{1,2} = \pm\|\mathbf{u}_0\|^2$. When the amplitude of the unperturbed modulation is vanishing, $\|\mathbf{u}_0\| = 0$, the equation (32) formally coincides with that of the Jeffcott rotor and therefore its eigenvalues are pure imaginary: $\lambda(k) = \pm i\alpha\sigma(\sigma \pm 2k)$. The eigencurves $\lambda(k)$ exhibit crossings at *diabolical points* [85] where double semi-simple eigenvalues originate.

What looks a bit more surprising is that at $\|\mathbf{u}_0\| \neq 0$ the spectrum of the gyroscopic system with the traceless indefinite 'damping' matrix (32) remains Hamiltonian [90], i.e. symmetric with respect to both real and imaginary axis of the complex plane[13]. At small amplitudes of the modulation, the eigenvalues are pure imaginary. With the increase in the amplitude, the modes with the opposite Krein signature collide at the threshold $\|\mathbf{u}_0\| = \|\mathbf{u}_0\|_i$, where $\|\mathbf{u}_0\|_i^2 = \frac{\alpha\sigma^2}{2\gamma}$ [83, 86]. At $\|\mathbf{u}_0\| > \|\mathbf{u}_0\|_i$ the doublet splits into complex-conjugate eigenvalues, one of which with positive real part, that corresponds to the modulational instability in the ideal (undamped) case that allows us to treat the modulational instability as the destabilization of a gyroscopic system by the indefinite damping [90, 95]. This destabilization mechanism is well known in rotor dynamics, where the indefinite damping matrix produced by the falling dependence of the friction coefficient on the sliding velocity, provokes vibrations in rotating elastic continua in frictional contact, e.g. in the singing wine glass [91, 92, 95].

When additional losses are taken into account, the interval of stability of the $\mathcal{PT}$-symmetric indefinitely damped gyroscopic system (32) can quite counter-intuitively be decreased, i.e. dissipation can *destabilize* the modulational instability [83, 87]. This is a manifestation of one of the most fundamental phenomena that characterize the non-conservative systems – the effect of *dissipation-induced instabilities* [93, 94]. In the last section we examine a non-conservative version of the Brouwer's problem from this perspective.

3.6 Non-conservative Brouwer's system

In 1976 Bottema [6] extended Brouwer's original setting by taking into account the internal and external damping with the coefficients δ and ν, respectively

$$\ddot{\mathbf{z}} + \mathbf{D}\dot{\mathbf{z}} + 2\Omega\mathbf{G}\dot{\mathbf{z}} + (\mathbf{K} + (\Omega\mathbf{G})^2)\mathbf{z} + \nu\mathbf{N}\mathbf{z} = 0 \tag{33}$$

with $\mathbf{z}^T = (x, y)$, $\mathbf{D} = \mathrm{diag}\,(\delta{+}\nu, \delta{+}\nu)$, $\mathbf{G} = \mathbf{J}$, $\mathbf{K} = \mathrm{diag}\,(k_1, k_2)$, and $\mathbf{N} = \Omega\mathbf{J}$. Eq. (33) appeared originally in the 1933 work by Smith [52] as a model of a rotor carried by a flexible shaft in flexible bearings, where the *stationary* (in the laboratory frame) damping coefficient ν represents the effect of viscous damping in bearing supports while the *rotating* damping coefficient δ represents the effect of viscous damping in the shaft [43]. The two types of damping were introduced in 1925 by Kimball [96] in order to explain a new type of supercritical instability encountered in built-up rotors in the early 1920s.

Quite in agreement with Prandtl [40], Smith concluded that when $\delta = 0$ and $\nu = 0$, the asymmetry of the bearing stiffness ($k_1 \neq k_2$) increases the interval of divergence instability (14) so that the second speed of transition from divergence to stability is higher (*supercritical*) than the critical speed $|\Omega| = \sqrt{k}$ of the perfectly symmetric rotor with $k_1 = k_2 = k$. Another Smith's conclusion sounded counter-intuitive: The speed of re-appearing of stability becomes larger also with the increase of asymmetry in the intensity of external damping relative to internal damping and this threshold speed is always supercritical [52]. In 1939 Kapitsa[14] encountered such destabilizing combinations of internal and external damping that complicated transition to supercritical speeds in a special high-efficiency expansion turbine that he developed for liquefaction of air [97].

[13] Note that the Hamiltonian form of the NLS equation is well-known [83, 84, 86]. Eq. (32) is also $\mathcal{PT}$-symmetric, i.e. invariant under transformations $t \leftrightarrow -t$ and $v_1 \leftrightarrow v_2$ [87].

[14] Pyotr Leonidovich Kapitsa (1894–1984) – a Russian physicist, for his experiments with liquid helium awarded the Nobel Prize in Physics in 1978.

In mechanics the forces with the skew-symmetric matrix $\mathbf{N}$ in Eq. (33) are referred to as *non-conservative positional* or *circulatory* [98]. Together with the velocity-dependent dissipation with the symmetric matrix $\mathbf{D}$, they constitute two fundamental *non-conservative forces* [99] that are responsible for many paradoxical stabilization and destabilization effects [94].

Let us assume that the damping matrix in Eq. (33) is $\mathbf{D} = \mathrm{diag}\,(\delta_1, \delta_2)$ and neglect the effect of non-conservative positional forces [100] Although the literal meaning of the word 'damping' prescribes the coefficients δ_1 and δ_2 to be non-negative, it is instructive to act similarly to as Brouwer did with respect to the stiffness coefficients k_1 and k_2 and relax this sign convention. Then, the negative damping coefficient corresponds to a gain and the positive one to a loss in the system [89].

In mechanics, negative damping terms enter the equations of motion of moving continua in frictional contact when the dependence of the frictional coefficient on the relative velocity has a negative slope, which can be observed already in the table-top experiments with the singing wine glass [91,92]. In physics, a pair of coupled oscillators, one with gain and the other with loss can naturally be implemented as an LRC-circuit [102] or as an optical system [103].

When $\delta_1 = -\delta_2 = \delta > 0$ the gain and loss in Eq. (33) are in a perfect balance. Let us further assume that $k_1 = k_2 = k$ and consider the dissipative Brouwer's equations in this special case Then, they are invariant with respect to the combined parity-time $(\mathcal{PT})$-transformation despite the $\mathcal{T}$-symmetry and $\mathcal{P}$-symmetry are not respected separately. The spectrum of the $\mathcal{PT}$*-symmetric* [88] system (33) with the *indefinite damping* is symmetrical with respect to the imaginary axis on the complex plane as it happens in Hamiltonian systems [90].

To see this, let us consider the eigenvalues λ of the problem (33) introducing the new parameters $X = \delta_1 + \delta_2$, $Y = \delta_1 - \delta_2$ and $\kappa = k_2 - k_1$. Then, at $X = 0$ and $\kappa = 0$ they represent the spectrum of the $\mathcal{PT}$-symmetric problem Eq. (33)

$$\lambda = \pm\frac{1}{4}\sqrt{2Y^2 - 16k_1 - 48\Omega^2 \pm 2\sqrt{(16\Omega^2 - Y^2)(32\Omega^2 + 16k_1 - Y^2)}}, \tag{34}$$

where $k_1 = k$ and $Y = 2\delta$. The eigenvalues (34) are pure imaginary when $|Y| < 4|\Omega|$. At the exceptional points (EPs), $Y = \pm 4\Omega$, the pure imaginary eigenvalues collide into a double defective one which with the further increase in Y splits into a complex conjugate pair (flutter instability).

The $\mathcal{PT}$-symmetry can be violated both by the asymmetry in the stiffness distribution $(\kappa \neq 0)$ and in the balance of gain and loss $(X \neq 0)$. Then, the Routh-Hurwitz conditions applied to the characteristic

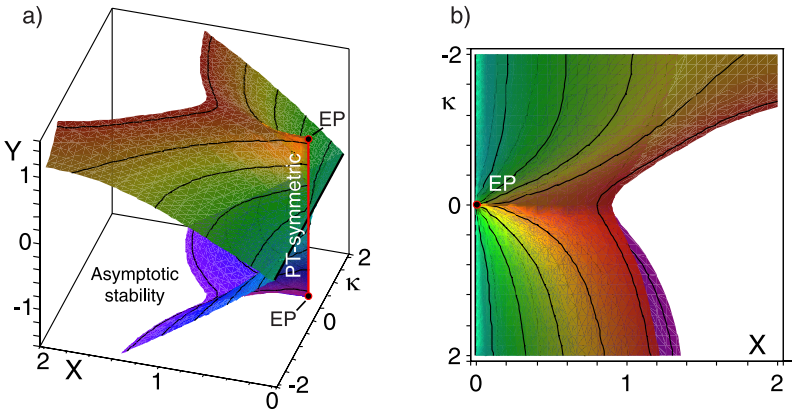

Fig. 9 (online colour at: www.fp-journal.org) (a) The boundary of the asymptotic stability of the system (33) plotted for $k_1 = 1$ and $\Omega = 0.3$ in the (κ, X, Y) space is locally equivalent to the Plücker conoid of degree $n = 1$. (b) The top view of the surface [87].

polynomial of such a system yield the boundary of the domain of the asymptotic stability that is shown in Fig. 9. In the (κ, X, Y) space the interval of marginal stability $|Y| < 4|\Omega|$ forms a singular edge of the stability boundary of the system with the violated $\mathcal{PT}$-symmetry, Fig. 9(a). The endpoints of the interval are EPs corresponding to the double pure imaginary eigenvalues with geometric multiplicity one. At the EPs the stability boundary has the Whitney umbrella singularity [87].

In the vicinity of the interval of the marginal stability of the $\mathcal{PT}$-symmetric system, the linear approximation to the boundary of the domain of the asymptotic stability is given by a *ruled surface* with the rulers

$$\kappa = -\frac{Y^2 - 16\Omega^2 \pm \sqrt{(Y^2 - 16\Omega^2)(Y^2 - 16k_1 - 32\Omega^2)}}{4Y} X. \tag{35}$$

A simple approximation for the threshold value of Y follows from Eq. (35)

$$Y \simeq \frac{4\Omega X\sqrt{k_1 + \Omega^2}}{\sqrt{\kappa^2 + X^2(k_1 + \Omega^2)}}. \tag{36}$$

Introducing the polar coordinates (ρ, ϕ) as $X\sqrt{k_1 + \Omega^2} = \rho\cos\phi$ and $\kappa = \rho\sin\phi$, we find a parametric representation of the surface (36)

$$(\rho, \phi) \mapsto \left(\frac{\rho}{\sqrt{k_1 + \Omega^2}}\cos\phi, \rho\sin\phi, 4\Omega\cos\phi\right). \tag{37}$$

This is a canonical form for the *Plücker conoid* surface of degree $n = 1$ [87].

Therefore, the threshold of asymptotic stability shown in Fig. 9 is locally equivalent to the Plücker conoid of degree $n = 1$, which is a singular surface with two self-intersections and two Whitney umbrella singular points.

In the plane $\kappa = 0$ the critical value of the parameter Y is growing with the increase of the parameter X that detunes the gain/loss balance, Fig. 10(a). Indeed, in this slice the boundary of the domain of the asymptotic stability is the hyperbola

$$Y^2 - X^2 = 16\Omega^2. \tag{38}$$

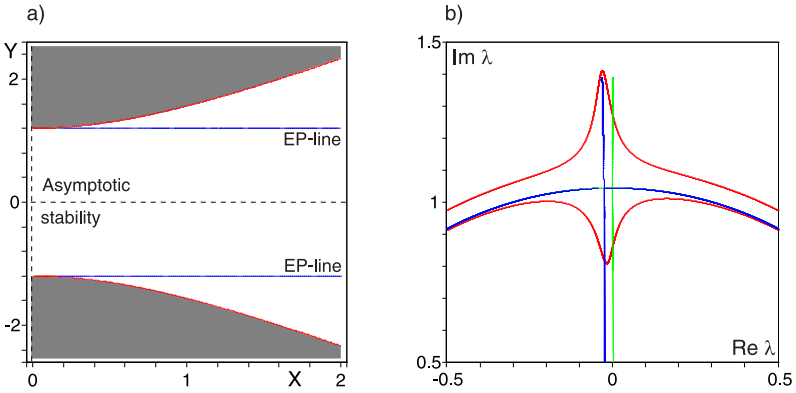

Fig. 10 (online colour at: www.fp-journal.org) (a) The boundary of the asymptotic stability and the set of complex EPs inside the stability domain for $k_1 = 1$, $\kappa = 0$, $\Omega = 0.3$. (b) The movement of eigenvalues in the complex plane as Y is varying in case when (green) the system is $\mathcal{PT}$-symmetric, (blue) $\kappa = 0$ and $X = 0.1$ and (red) $\kappa = 0.1$ and $X = 0.1$.

At $X = 0$ it touches the two straight lines $Y = \pm 4\Omega$ every point of which corresponds to a pair of double defective complex conjugate eigenvalues with real parts negative when $X > 0$, positive when $X < 0$ and zero when $X = 0$

$$\lambda = -\frac{X}{4} \pm \frac{1}{4}\sqrt{X^2 - 16(k_1 - \Omega^2)}. \tag{39}$$

The two EP-lines stem from the end points of the stability interval of the $\mathcal{PT}$-symmetric system and continue inside the asymptotic stability domain of the imperfect one, see Fig. 10(a).

The proximity of a set of the defective eigenvalues to the boundary of the asymptotic stability that generically is characterized by simple pure imaginary eigenvalues plays an important role in modern non-conservative physical and mechanical problems. For example, near this set the eigenvalues can dramatically change their trajectories in the complex plane [104]. By this reason, encountering the EPs with the negative real parts was considered as a precursor to the oscillatory instability in the studies of electrical networks [105], hydrodynamical flows [104], and friction-induced oscillations [101], see also [87].

Indeed, in the complex plane the eigenvalues of the ideal system with $X = 0$ and $\kappa = 0$ demonstrate the Krein collision on the imaginary axis shown in green in Fig. 10(b). When $X > 0$, the complex eigenvalues with negative real parts collide to the left of the imaginary axis at an EP. This 'strong modal resonance' [105] is shown in blue lines in Fig. 10(b). It is indeed a precursor to flutter instability because after the interaction one of the eigenvalues moves to the right and crosses the imaginary axis at a higher value of Y. In the presence of stiffness detuning ($\kappa \neq 0$), the merging of eigenvalues becomes imperfect. The characteristic pattern of the imperfect merging of modes shown as red lines in Fig. 10(b), occurs in the vicinity of the EP-set of Fig. 10(a) and by this reason it still indicates the proximity of flutter. At $X < 0$ the set of EPs corresponds to the complex eigenvalues with positive real parts and lies in the instability domain. A similar situation may take place in optics where the EPs can exist above the lasing threshold [106].

Conclusion

Completing this short excursion into the mechanics of diabolical and exceptional points we hope that it will attract attention of physicists to the well developed spectral methods of applied mathematics and theoretical mechanics that were motivated mostly by the stability problems. On the other hand, the quickly growing non-Hermitian physics and the new mathematical achievements accompanying this process should not pass by those who works on the modern non-conservative problems of solid and fluid mechanics. The prospects of such a synthesis look especially fortunate in light of that, as our survey demonstrates, numerous so different at first sight phenomena can frequently lead to literally the same dynamical systems.

References

[1] D. F. Moyer, Stud. Hist. Philos. Sci. A **8**, 251 (1977).
[2] M. V. Berry, Czech. J. Phys. **54**, 1039 (2004).
[3] W. D. Heiss, Czech. J. Phys. **54**, 1091 (2004).
[4] I. Rotter, J. Phys. A-Math. Theor. **42**, 153001 (2009).
[5] B. Dietz et al., Phys. Rev. Lett. **106**, 150403 (2011).
[6] O. Bottema, Z. Angew. Math. Phys. **27**, 663 (1976).
[7] L. E. J. Brouwer, N. Arch. v. Wisk. **2**, 407 (1918).
[8] F. J. W. Whipple, Philos. Mag., 6th Ser. **33**, 457 (1917).
[9] R. Hryniv and P. Lancaster, Z. Angew. Math. Mech. **81**, 675 (2001).
[10] K. Huseyin, J. Sound Vib. **45**, 29 (1976).
[11] D. Afolabi, J. Sound Vib. **182**, 229 (1995).
[12] P. Gallina, J. Sound Vib. **262**, 977 (2003).
[13] R. S. MacKay, in: Nonlinear Phenomena and Chaos, edited by S. Sarkar (Adam Hilger, Bristol, 1986), p. 254.

[14] T. Kato, Perturbation Theory for Linear Operators (Springer, Berlin, 1980).
[15] J. Moro, J. V. Burke, and M. L. Overton, SIAM J. Matrix Anal. Appl. **18**, 793 (1997).
[16] P. Binding and H. Volkmer, SIAM Rev. **38**, 27 (1996).
[17] K. Huseyin, Vibrations and Stability of Multiple Parameter Systems (Kluwer, Dordrecht, The Netherlands, 1978).
[18] V. V. Kozlov, Gyroscopic stabilization and parametric resonance, PMM J. Appl. Math. Mech. **65**, 715 (2001).
[19] R. I. Thompson, T. J. Harmon, and M. G. Ball, Can. J. Phys. **80**, 1433 (2002).
[20] I. Gohberg, P. Lancaster, and L. Rodman, Matrix Polynomials (Academic Press, San Diego, CA, 1982).
[21] M. V. Keldysh, Dokl. Akad. Nauk SSSR **77**, 11 (1951).
[22] G. W. Stewart and J. G. Sun, Matrix Perturbation Theory (Academic Press, Boston, 1990).
[23] M. G. Krein, Topics in Differential and Integral Equations and Operator Theory (Birkhäuser, Basel, 1983).
[24] P. J. Morrison, Rev. Mod. Phys. **70**, 467 (1998).
[25] J. van der Meer, Hamiltonian Hopf Bifurcation, in: Lect. Notes Math. Vol. 1160 (Springer-Verlag, Berlin, 1985).
[26] M. Dellnitz, I. Melbourne, and J. E. Marsden, Nonlinearity **5**, 979 (1992).
[27] B. Cushman-Roisin, Geophys. Astrophys. Fluid. Dyn. **22**, 85 (1982).
[28] N. Paldor and A. Sigalov, Phys. D **160**, 29 (2001).
[29] M. Levi, The Mathematical Mechanic: Using Physical Reasoning to Solve Problems (Princeton University Press, Princeton, NJ, 2009).
[30] V. I. Arnold, Russ. Math. Surv. **26**, 29 (1971).
[31] O. N. Kirillov, D. E. Pelinovsky, and G. Schneider, Phys. Rev. E **84**, 065301(R) (2011).
[32] O. N. Kirillov, Phys. Lett. A **375**, 1653 (2011).
[33] D. J. Inman, Trans. ASME E, J. Appl. Mech. **55**, 895 (1988).
[34] A. Seyranian and A. Mailybaev, Multiparameter Stability Theory with Mechanical Applications (World Scientific, Singapore, 2003).
[35] G. G. Denisov, V. V. Novikov, and A. E. Fedorov, Trans. ASME E, J. Appl. Mech. **77**, 031017 (2010).
[36] K. Veselic, Z. Angew. Math. Mech. **75**, 325 (1995).
[37] W. J. M. Rankine, The Engineer **27**, 249 (1869).
[38] A. Föppl, Der Civilingenieur **41**, 333 (1895).
[39] T. von Karman, in: Encyklopaedie der Mathematischen Wissenschaften, IV:4, ch. Festigkeitsprobleme im Maschinenbau (Teubner, Leipzig, 1910) p. 311.
[40] L. Prandtl, Dinglers Polytechn. J. **20**, 179 (1918).
[41] H. H. Jeffcott, Philos. Mag. Ser. **6**(37), 304 (1919).
[42] A. M. Bloch, P. Hagerty, A. G. Rojo, and M. I. Weinstein, J. Stat. Phys. **115**, 1073 (2004).
[43] S. H. Crandall, J. Sound Vib. **11**, 3 (1970).
[44] S. H. Crandall, Z. Angew. Math. Phys. **46**, S761 (1995).
[45] V. Apostolyuk and F. E. H. Tay, Sensor Lett. **2**, 252 (2004).
[46] G. Bryan, Proc. Camb. Philos. Soc. **7**, 101 (1890).
[47] M. Y. Shatalov, A. G. Every, and A. S. Yenwong-Fai, Int. J. Solids Struct. **46**, 837 (2009).
[48] U. Nackenhorst and M. Brinkmeier, Arch. Appl. Mech. **78**, 477 (2008).
[49] J. Baillieul and M. Levi, Arch. Ration. Mech. Anal. **115**, 101 (1991).
[50] W. Kerr, Engineering **101**, 150 (1916).
[51] F. C. Nelson, Sound Vib. **37**(6), 8 (2003).
[52] D. M. Smith, Proc. R. Soc. Lond. A **142**, 92 (1933).
[53] W. Campbell, Trans. ASME **46**, 31 (1924).
[54] C. W. Roberson, A. Mondelli, and D. Chernin, Phys. Rev. Lett. **50**, 507 (1983).
[55] V. E. Shapiro, Phys. Lett. A **290**, 288 (2001).
[56] V. I. Arnold, Mathematical Methods of Classical Mechanics (Springer, Berlin, 1989).
[57] M. I. Krivoruchenko, Phys.-Usp. **52**, 821 (2009).
[58] R. S. MacKay and J. A. Sepulchre, Physica D **119**, 148 (1998).
[59] S. B. Andersson and P. S. Krishaprasad, The Hannay-Berry Phase of the Vibrating Ring Gyroscope, Technical Research Report no. CDCSS TR 2004-2, (University of Maryland, College Park, 2004).
[60] S. V. Joubert, M. Y. Shatalov, and T. H. Fay, Am. J. Phys. **77**, 520 (2009).
[61] S. B. Andersson, Geometric Phases in Sensing and Control, Ph.D. thesis, (Univ. Maryland, College Park, 2003).

[62] J. E. Marsden, R. Montgomery, and T. Ratiu, Mem. Am. Math. Soc. **88**, 1 (1990).
[63] J. E. Marsden, O. M. O'Reilly, F. J. Wicklin, and B. W. Zombro, Nonlinear Sci. Today **1**, 14 (1991).
[64] M. V. Berry, Proc.R. Soc. Lond. A **392**, 45 (1984).
[65] J. H. Hannay, J. Phys. A, Math. Gen. **18** (1985).
[66] K. Y. Bliokh, J. Opt. A **11**, 094009 (2009).
[67] K. Y. Bliokh et al., Rev. Mod. Phys. **80**, 1201 (2008).
[68] K. Y. Bliokh, Y. Gorodetski, V. Kleiner, and E. Hasman, Phys. Rev. Lett. **101** (2008).
[69] K. Y. Bliokh, A. Niv, V. Kleiner, and E. Hasman, Nature Photon. **2**, 748 (2008).
[70] S. G. Lipson, Opt. Lett. **15**, 154 (1990).
[71] A. S. Marathay, Opt. Commun. **3**, 369 (1971).
[72] F. S. Chute, F. E. Vermeulen, and E. A. Youssef, Nucl. Instrum. Methods **82**, 86 (1970).
[73] E. A. Youssef, F. S. Chute, and F. E. Vermeulen, Nucl. Instrum. Methods **93**, 181 (1971).
[74] V. Antropov et al., Nucl. Instrum. Methods, Phys. Res. A **532**, 172 (2004).
[75] F. M. Penning, Physica **3**, 873 (1936).
[76] W. Paul, Rev. Mod. Phys. **62**, 531 (1990).
[77] R. M. Pearce, Nucl. Instrum. Methods **83**, 101 (1970).
[78] N. R. Lebovitz and E. Zweibel, Astrophys. J. **609**, 301 (2004).
[79] M. V. Berry and P. Shukla, Eur. J. Phys. **32**, 115 (2011).
[80] Y. S. Kivshar and M. Peyrard, Phys. Rev. A **46**, 3198 (1992).
[81] T. B. Benjamin and J. E. Feir, J. Fluid Mech. **27**, 417 (1967).
[82] V. Bespalov and V. Talanov, JETP-Lett. USSR **3**, 307 (1966).
[83] T. J. Bridges and F. Dias, Phys. Fluids **19**, 104104 (2007).
[84] V. E. Zakharov, J. Appl. Mech. Tech. Phys. **9**, 190 (1968).
[85] O. N. Kirillov, A. A. Mailybaev, and A. P. Seyranian, J. Phys. A, Math. Gen. **38**, 5531 (2005).
[86] V. E. Zakharov and L. A. Ostrovsky, Physica D **238**, 540 (2009).
[87] O. N. Kirillov, Phys. Lett. A **376**, 1244 (2012).
[88] C. M. Bender and P. D. Mannheim, Phys. Lett. A **374**, 1616 (2010).
[89] P. Freitas, M. Grinfeld, and P. A. Knight, Adv. Math. Sci. Appl. **17**, 435 (1997).
[90] P. Freitas, Z. Angew. Math. Phys. **50**, 64 (1999).
[91] O. N. Kirillov, Proc. R. Soc. Lond. A **464**, 2321 (2008).
[92] O. N. Kirillov, Proc. R. Soc. Lond. A **465**, 2703 (2009).
[93] A. M. Bloch, P. S. Krishnaprasad, J. E. Marsden, and T. S. Ratiu, Ann. Inst. Henri Poincare **11**, 37 (1994).
[94] O. N. Kirillov and F. Verhulst, Z. Angew. Math. Mech. **90**, 462 (2010).
[95] W. Kliem and C. Pommer, Z. Angew. Math. Phys. **60**, 785 (2009).
[96] A. L. Kimball, Philos. Mag. **49**, 724 (1925).
[97] P. L. Kapitsa, Zh. Tech. Phys. **9**, 124 (1939).
[98] H. Ziegler, Z. Angew. Math. Phys. **4**, 89 (1953).
[99] R. Krechetnikov and J. E. Marsden, Physica D **214**, 25 (2006).
[100] R. C. Shieh and E. F. Masur, Z. Angew. Math. Phys. **19**, 927 (1968).
[101] J.-J. Sinou, F. Thouverez, and L. Jezequel, Comput. Struct. **84**, 1891 (2006).
[102] J. Schindler et al., Phys. Rev. A **84**, 040101(R) (2011).
[103] C. E. Ruter et al., Nature Phys. **6**, 192 (2010).
[104] C. A. Jones, Q.J. Mech. Appl. Math. **41**, 363 (1988).
[105] I. Dobson et al. IEEE Trans. Circ. Syst. I **48**, 340 (2001).
[106] M. Liertzer et al., Phys. Rev. Lett. **108**, 173901 (2012).

